Chemical Science

EDGE ARTICLE

View Article Online
View Journal | View Issue

Cite this: *Chem. Sci.*, 2015, **6**, 2102

Light-induced crosslinkable semiconducting polymer dots†

Yue Zhang, Fangmao Ye, Wei Sun, Jiangbo Yu, I-Che Wu, Yu Rong, Yong Zhang and Daniel T. Chiu*

Received 20th December 2014
Accepted 23rd January 2015

DOI: 10.1039/c4sc03959a

www.rsc.org/chemicalscience

This paper describes a synthetic approach for photocrosslinkable polyfluorene (pc-PFO) semiconducting polymer dots, and demonstrates their superior ability to crosslink and form 3-D intermolecular polymer networks. The crosslinked pc-PFO Pdots are equipped with excellent encapsulating ability of functional small molecules. Optimum conditions of light irradiation on pc-PFO Pdots were investigated and clarified by using polymer thin films as a model. By employing the optimal light irradiation conditions, we successfully crosslinked pc-PFO Pdots and studied their particle sizes, photophysical, and colloidal properties. Single-particle imaging and dynamic-light-scattering measurements were conducted to understand the behaviors of photocrosslinked Pdots. Our results indicate pc-PFO Pdots can be easily photocrosslinked and the crosslinked species have excellent colloidal stability, physical and chemical stability, fluorescence brightness, and specific binding properties for cellular labeling. Considering that optical stimulus can work remotely, cleanly, and non-invasively, this study should pave the way for a promising approach to further develop stimuli-responsive ultrabright and versatile Pdot probes for biomedical imaging.

Introduction

Semiconducting polymer dots (Pdots) are emerging as useful tools for fluorescence probing due to their high brightness, fast emission rates, and non-blinking and non-toxic features.[1–11] These excellent characteristics make Pdots promising fluorescent cellular labels for flow cytometry,[3,12] specific cellular[2,13] and subcellular[14] imaging, and *in vivo* imaging.[12,15–18] Pdots composed of π-conjugated hydrophobic polymers are characterized by small particle sizes (∼<30 nm) and a higher than 50%, preferably 80–90% volume fraction or weight concentration.[5] Small particle size is an important feature as it can offer better tissue and subcellular penetration while minimizing non-specific interaction.[14,19] Recent research demonstrates that single-particle brightness and cell-labeling brightness of Pdots are more than an order of magnitude higher than those of inorganic Qdots with comparable particle sizes or three orders of magnitude higher than organic dyes.[3,12,20] Such extraordinary brightness stimulated researchers to explore more functions of Pdots as fluorescence labels. There have been significant efforts to develop versatile and robust Pdots with various properties and functions, such as stimuli responsive Pdots that can detect pH,[21] temperature,[22] or concentration of metal ions.[7,23]

Among various external stimuli, optical stimulus is especially attractive as it can work cleanly and non-invasively, as well as allowing remote biomedical treatment. Chan *et al.* reported photoswitchable Pdots by mixing photo-sensitive small molecules and studied their reversible photo-switchability of fluorescence emission by UV and visible light irradiation.[24] In addition, Pu *et al.* reported a near-infrared light-absorbing semiconducting polymer nanoparticles that can convert photons to ultrasound waves and allow *in vivo* photoacoustic imaging.[4] These are encouraging achievements of optical manipulation on polymer nanoparticles, which stimulate the exploration of potential novel functionalities of fluorescent probes and the development of new bio-imaging techniques. Therefore, developing photo-stimuli responsive Pdots is important and promising for introducing novel functions in Pdots.

Here, we describe a photocrosslinking strategy to crosslink semiconducting polymers in Pdots dispersed in aqueous solution induced by UV-light irradiation (Fig. 1). Photo-induced crosslinking of Pdots results in enhanced colloidal stability of Pdots in aqueous solution, especially when they come into contact with detergents or organic solvents, and also can provide physically and chemically-stable crosslinked 3D nano-sized structures for efficient encapsulation and storage of functional materials.

Department of Chemistry, University of Washington, Seattle, Washington 98195, USA. E-mail: chiu@chem.washington.edu

† Electronic supplementary information (ESI) available: Synthesis and characterization of monomers and polymers, preparation and characterization of thin film and Pdots, optical property measurements and flow cytometry is available. See DOI: 10.1039/c4sc03959a

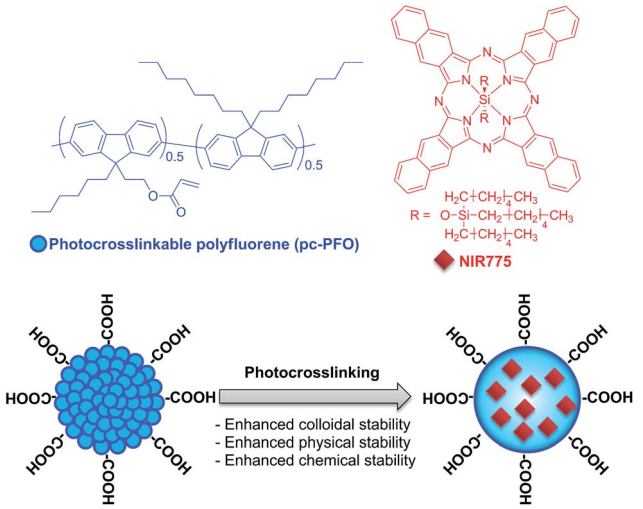

Fig. 1 Schematic showing the chemical structures of the photocrosslinkable Pdots used in this study and the NIR dye used for demonstrating stable small-molecule encapsulation into crosslinked Pdots.

As for reported chemical crosslinking methods in conjugated polymer nanoparticles, Hittinger *et al.* used palladium-catalyst cross-coupling reaction to synthesize crosslinked conjugated polymer nanoparticles, with the particle sizes ranging from 50 nm to 10 μm.[25] In addition, Zhou *et al.* synthesized conjugated polymer nanoparticles (40–210 nm) with numerous surface hydroxyl groups by dendritic crosslinking with copper free click chemistry, and the obtained nanoparticles showed stable fluorescence, good photostability and low cytotoxicity for cell labeling and imaging.[26] Furthermore, Yu *et al.* reported another chemical treatment method by covalently binding functional small molecules to Pdots, and successfully obtained stable functionalized Pdots with very small sizes (<10 nm), which is useful in labeling cell surface receptors and subcellular microtubules for fluorescence imaging.[19] All of these reported methods employed chemical reactions in the synthesis of cross-linked polymer nanoparticles, which include various transition metal or nucleophilic catalysts as well as organic solvents for the preparation of crosslinked polymer nanoparticles. Compared to these previous reports, our method utilizes a clean and remote external stimulus – light.

In this report, we inserted photocrosslinkable side chains into the semiconducting polymer backbone, which worked as photo-active crosslinkers. These crosslinkers react with each other upon UV light irradiation, and therefore bond covalently to form an intermolecular crosslinked 3D polymer network. The irradiation time is optimized by using semiconducting polymer thin films as a model system, in which we characterized the degree of crosslinking by measuring the residual percentages of photocrosslinked thin films after immersion in organic solvents as detected by UV-vis spectra. Pdots were then photocrosslinked with the optimal irradiation time, and their morphology, colloidal and optical properties were characterized thoroughly.

To study the photocrosslinked Pdots, we employed single-particle fluorescence imaging and dynamic light scattering (DLS) measurement to observe the Pdots. Without photocrosslinking, Pdots dispersed on glass substrate can be easily washed off after immersion in tetrahydrofuran (THF) as visualized in single-particle imaging. In contrast, photocrosslinked Pdots form insoluble crosslinked 3D polymer network, and thus can still remain on the substrate after THF wash. In addition, DLS measurements provided clear evidence of stable particle sizes in photocrosslinked Pdots even after exposure to organic solutions. We show such structurally stable Pdots with enhanced colloidal stability[19] act as efficient small molecule capsules with greatly minimized leakage when compared with regular Pdots. We also applied the photocrosslinked Pdots to label the surface of breast cancer cells to illustrate their performance in flow cytometry experiments, and to demonstrate their ability in achieving high labeling efficiency and sensitivity in biological assays.

Results and discussion

Synthesis and characterization

Schemes S1 and S2† show the synthetic routes for monomer and the photocrosslinkable polyfluorene semiconducting polymer (pc-PFO), with the detailed synthetic procedures described in Experimental section. In monomer synthesis, the methoxyalkyl substituents attached to the fluorescent monomer were synthesized in THF by adding in a stepwise fashion methoxyalkyl bromide and alkyl bromide. Note that substitution reaction of methoxy alkyl bromide in ether solvent as reported in the literature introduces two instead of one methoxyalkyl chains in one fluorene ring at the same time. The asymmetric methoxyalkylfluorene was then brominated by excess amount of bromine and purified for polymerization. The polymer precursor P1 was prepared *via* Suzuki polycondensation reaction in a biphasic system (toluene/aqueous Na_2CO_3) using fresh $Pd(PPh_3)_4$ as a catalyst. Note that polymerization should have Freeze–Pump–Thaw (FPT) cycling for 2–3 times before increasing to 90 °C for polymerization. This procedure can reduce oxygen to a much lower level and maintain consistent chemical environments each time when loading and performing a chemical reaction.

Gel permeation chromatography (GPC) analysis indicated that the molecular weight (M_n) and the polydispersity index (PDI) of polymer P1 are 25k and 1.9, respectively. Polymer P1 showed excellent solubility in common organic solvents such as THF, toluene, chloroform and dichloromethane. With the treatment of boron tribromide, the methoxy group was easily removed from the side chains of polymer to give polymer precursor P2. This P2 could be clearly observed from proton NMR spectrum, as the signal of methoxy groups disappeared in P2. P2 was not as soluble as P1 in common organic solvents, and tended to aggregate in THF or dichloromethane. Thermal treatment above 50 °C helped to increase the solubility in those organic solvents. Finally, the photocrosslinkable acrylate group was introduced in the side chains of polymer by adding acryloyl chloride to get target polymer pc-PFO. The acrylation reaction

was conducted in the dark and worked up in a short time to prevent any photochemical reactions. pc-PFO showed better solubility than P2, and thermal treatment helped to increase solubility in organic solvents as well. However, filtration through PVDF filters with 0.2 μm pore size was necessary to remove large aggregations in solutions before further processing. Note that photocrosslinkable acrylate group was introduced after Suzuki coupling reaction to avoid unnecessary side reactions.

Optimization of UV-light irradiation time by using thin films

Thin film is one type of solid state in polymeric materials, and provides a convenient model to approximate the chemical environments in Pdots. Thus, optimization of irradiation time using polymer pc-PFO thin films can afford useful information for photocrosslinking reactions in pc-PFO Pdots. The crosslinkability of polymer pc-PFO by UV-light irradiation was investigated based on the insolubility of the crosslinked thin films in organic solvents, as monitored by UV-vis absorption spectra.

pc-PFO thin films were prepared by spin-coating 5 mg mL^{-1} chloroform solution of pc-PFO on pre-washed glass substrates, followed by UV-light irradiation for different durations, ranging from 10 s to 120 min for the photocrosslinking reaction. The irradiation was conducted using a 365 nm UV lamp light source with a power of 0.35 mW cm^{-2}. UV-vis spectra of thin films were measured before and after the photocrosslinking reaction, and after which the thin films were immersed into THF for 30 min at 50 °C. Thermal treatment can increase the solubility of polymer in THF and remove uncrosslinked pc-PFO thin films thoroughly. After the samples were completely dried, UV-vis spectra were taken again to determine the amount of polymers that remained on the glass substrate. We note the thickness of the polymer film was about 10–20 nm, which was quite close to the particle sizes of Pdots. Thus, we believe light irradiation conditions on thin films of conjugated polymers should be quite similar to that for Pdots.

Fig. S1(a–h)† shows UV-vis absorption spectra of pc-PFO thin films with different irradiation times, which were collected before (black line) and after (blue line) light exposure, and after solvent immersion (red line). Note that pc-PFO thin films with different irradiation times were prepared separately but using identical procedure to ensure constant film thickness. Fig. 2a and b shows a time series of photocrosslinking time *versus* percentages of pc-PFO thin film residues. Percent pc-PFO thin film residues were calculated by dividing the intensities of absorption peak (390 nm) of pc-PFO thin films after photocrosslinking and after immersion in THF by the intensity value before photocrosslinking (Fig. 2a and b). Monotonic decrease of percent residues in Fig. 2a indicated the photobleaching of polymer pc-PFO by UV-light irradiation due to the photochemical destruction of pc-PFO fluorophore. But irradiation times of up to 60 min could still maintain at least 80% of the absorption of pc-PFO thin films. After immersion in THF, uncrosslinked pc-PFO thin films were washed off from the substrate as they dissolved in THF solutions, which resulted in the percent residue

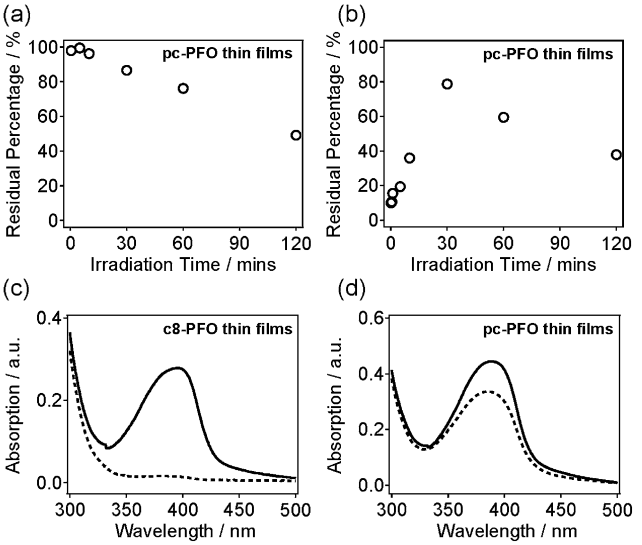

Fig. 2 Time series plots of photocrosslinking time *versus* pc-PFO thin-film residual percentages. The pc-PFO thin-film residual percentages were calculated by dividing the intensity of the absorption peak of pc-PFO thin films (a) after photocrosslinking and (b) after THF wash by the value before photocrosslinking. UV-vis absorption spectra of (c) uncrosslinked c8-PFO and (d) 30 min photocrosslinked pc-PFO spin-coated thin films before (solid line) and after (dashed line) the immersion and wash in THF.

to decrease even more (Fig. 2b). Irradiation for 30 min in pc-PFO thin films showed the best percent residue remaining on the substrate, suggesting 30 min was the optimal irradiation time for photocrosslinking of pc-PFO. In Fig. 2b, the increase in percent residues on the substrate from 10 s to 30 min was mainly caused by the increase of the crosslinking ratios, and the decrease from 30 min to 120 min was mainly from the photobleaching of pc-PFO thin films, respectively.

Thin films of commercial polydioctylfluorene (c8-PFO, M_n = 40 000–150 000) polymer were also prepared as a control. c8-PFO does not have photocrosslinking ability as there are no photo-sensitive chemical groups in its polymeric structure. Fig. 2c and d shows the UV-vis spectra of uncrosslinked c8-PFO and the 30 min irradiated pc-PFO thin films before and after THF immersion. In the c8-PFO film (Fig. 2c), no absorption was observed after THF immersion, indicating that c8-PFO was completely washed off from the substrate and dissolved into THF. In comparison with c8-PFO thin films, *ca.* 80% of the UV-vis absorption still remained in pc-PFO thin film after identical treatment (Fig. 2d). These results indicate pc-PFO was successfully photocrosslinked at the side chains attached to polyfluorene backbones and thus became insoluble in organic solvents.

To summarize, we found irradiation for 30 min was the optimal condition for photocrosslinking reaction in pc-PFO thin films. In the following experiments, we applied 30 min irradiation time for photocrosslinking reaction in pc-PFO Pdots, and compared the physical properties of pc-PFO and c8-PFO Pdots, as well as their bio-conjugation and cell labeling after photocrosslinking.

Pdots preparation and photocrosslinking reaction

Using the functionalized pc-PFO polymers as precursors, pc-PFO Pdots were prepared by rapid injection of the pc-PFO THF solution into water under vigorous ultrasonication. The Pdot-preparation details are described below in Experimental section. The Pdot sizes could be controlled by varying the precursor polymer concentration and the injection volume. In our experiments, the concentration and injection volume of the precursor polymer solution were fixed so as to keep a consistent particle size. The Pdot size was investigated by transmission electron microscopy (TEM) and DLS. Fig. 3 shows representative TEM and DLS data for the Pdots made from pc-PFO before and after photocrosslinking, as shown in the left and right panels in Fig. 3a and b, respectively. Pdots made from commercially available c8-PFO, which could not be photocrosslinked, were also prepared as a control and for comparison (Fig. 3c).

From DLS measurements, the particle sizes of pc-PFO and c8-PFO Pdots have comparable diameters of 18–19 nm, which were prepared by injecting polymer in THF solution (4 mL, 50 mg mL^{-1}) into 8 mL of H_2O under ultrasonication. TEM images showed relatively uniform particle sizes and shapes for both pc-PFO and c8-PFO Pdots. There were no obvious changes in particle size, particle shape, or zeta potential between before and after photocrosslinking for pc-PFO Pdots (Fig. 3a and b and Table 1). This indicates photocrosslinking at side chains of pc-PFO Pdots did not change the shape or surface properties of the nanoparticles. As expected, the control c8-PFO Pdots also showed no obvious changes in particle size, particle shape, or zeta potential between before and after irradiation (Fig. 3c and Table S1†) because c8-PFO lacked photocrosslinkable side chains. There is a potential for photocrosslinking to occur between Pdots, but we did not observe this in any of our experiments, most likely because the PEG–COOH groups from PS–PEG–COOH dominated the surface functional groups on Pdots, which caused the Pdot surface to be negatively charged and the Pdots to repel each other in aqueous solution.

For all our subsequent experiments, we prepared Pdots with particle sizes fixed at 18–19 nm to enable us to make meaningful comparisons when we studied their photophysical properties and cellular targeting capability. The irradiation was carried out using a 365 nm UV lamp light source with a power of 0.35 mW cm^{-2}, and under nitrogen bubbling to minimize photobleaching of the polymers.

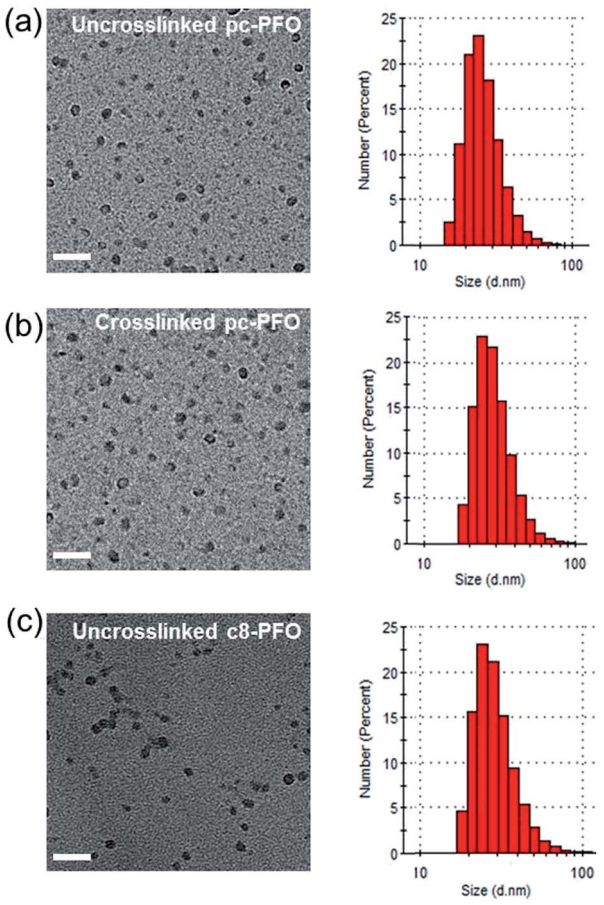

Fig. 3 Transmission-electron-microscopy images (left) and histograms showing the distribution of the sizes of Pdots as measured by dynamic-light-scattering (right) of (a) uncrosslinked pc-PFO Pdots; (b) 30 min photocrosslinked pc-PFO Pdots; (c) uncrosslinked c8-PFO Pdots. Scale bar: 100 nm.

Optical properties

Absorption and fluorescence spectroscopy were performed to investigate the optical properties of the pc-PFO Pdots before and after photocrosslinking. Non-photocrosslinkable c8-PFO Pdots were also prepared for comparison. Before photocrosslinking, c8-PFO Pdots showed better intermolecular π–π stacking than pc-PFO Pdots, indicated by the narrow, red-shifted and well-resolved absorption peak at 435 nm that was enhanced in c8-PFO Pdots (Fig. S2†). In addition, the fluorescence also displayed a narrow, red-shifted emission peak at 439 nm and a well-resolved vibronic progression in the emission spectrum. Both of these features in the absorption and emission spectra indicate the presence of β-phase in c8-PFO Pdots and thus good intermolecular π–π stacking.[27]

The absence of absorption shoulder in pc-PFO Pdots is likely caused by the steric hindrance of the bulky acrylate groups in the side chains of the pc-PFO polymer (Fig. S3a†). As seen in Fig. S3,† the pc-PFO Pdots exhibit quite similar absorption and fluorescence spectra profiles after photocrosslinking. Absorption peak of pc-PFO Pdots, however, blue-shifted *ca.* 6 nm after irradiation for 60 min, resulting from the photocrosslinking reaction in the side chains of pc-PFO polymer in Pdots. Double

Table 1 Size, zeta potential, and photophysical properties of pc-PFO Pdots with different UV-light irradiation times for photocrosslinking

	Uncrosslinked (not irradiated)	30 min	60 min
Size (nm)[a]	18	18	18
ζ (mV)[b]	−43	−43	−40
Φ (%)[c]	23 ± 1	17 ± 1	11 ± 2

[a] Hydrodynamic size. [b] Zeta potential. [c] Fluorescence quantum yield.

bonds of C=O and C=C opened to form a ring structure in 3D intermolecular networks after photocrosslinking. Formation of new chemical bonds in pc-PFO Pdots spatially constrained each polymer chain and increased steric hindrance of intermolecular π-packings between polyfluorene backbones. Thus UV-vis absorption shifted to shorter wavelengths, accompanied by a red-shift in fluorescence spectra (Fig. S3b†). However, even when Pdots got photocrosslinked the conformation of the polymer chains were most likely still fairly relaxed because of the flexible alkyl chain spacers attached to the rigid fluorene backbones, as reflected by the very small shifts of both absorption and fluorescence peaks. In contrast, UV-vis spectra and fluorescence spectra profiles of c8-PFO Pdots remained the same, confirming no structural changes after irradiation.

A negative effect caused by UV-light irradiation on pc-PFO Pdots was a reduction in fluorescence quantum yield (Table 1). The quantum yield of pc-PFO Pdots was 0.23 before light irradiation, but it decreased to 0.17 and to 0.11 after light irradiation for 30 and 60 min, respectively. This decrease was caused by photobleaching of some pc-PFO polymer as mentioned above. Given Pdots can be an order of magnitude brighter (up to 30×)[3] than Qdots, this ~25% reduction in quantum yield and thus brightness, is quite manageable. However, this reduction in brightness with increasing durations of light irradiation indicates there is an optimal irradiation time to achieve both high brightness and photocrosslinking in Pdots. Based on the results of pc-PFO thin films, we chose 30 min to be the optimal irradiation time for forming photocrosslinked Pdots; we used this irradiation time for all our subsequent experiments with photocrosslinked Pdots.

Validation of photocrosslinking in pc-PFO Pdots by DLS measurement and single-particle imaging

Fig. 4 shows the results of DLS measurements. The tested samples were uncrosslinked c8-PFO, uncrosslinked pc-PFO, and crosslinked pc-PFO Pdots. After Pdot preparation, various amounts of THF (10 vol% to 400 vol% with respect to the volume of the Pdot aqueous solution) were added to the Pdot aqueous solutions, followed by heating at 50 °C for 30 min to enhance the solubility of Pdots. After removal of THF, DLS measurements were conducted on the Pdot aqueous solutions. Uncrosslinked c8-PFO and uncrosslinked pc-PFO Pdots showed constant particle sizes of *ca.* 20 nm after adding up to 50 vol% THF, but then increased in size to nearly 80 nm when 100 vol% to 400 vol% of THF was added. These results indicate uncrosslinked Pdots were swelled and dissolved in THF and then re-precipitated after removal of THF to form either Pdots with larger particle sizes, or more likely polymer aggregates in aqueous solutions. In contrast, crosslinked pc-PFO showed constant particle sizes of *ca.* 20 nm no matter how much THF was added, indicating the photocrosslinked pc-PFO Pdots were highly stable and were not dissolved in THF.

Another evidence of photocrosslinking was obtained by using single-particle imaging. The Pdots were dispersed on pre-treated glass substrate at an appropriate concentration so we could resolve individual Pdots under single-particle imaging. Pdots have a negative surface charge as indicated by zeta potential measurements (Table 1 and S1†), thus glass substrate

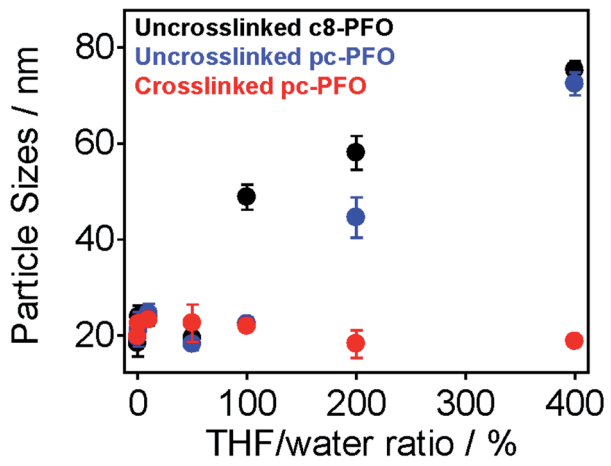

Fig. 4 Particle sizes and error bars of uncrosslinked c8-PFO (black), uncrosslinked pc-PFO (blue), and crosslinked pc-PFO (red) Pdots in aqueous solution after being swelled by various amounts of THF solvent.

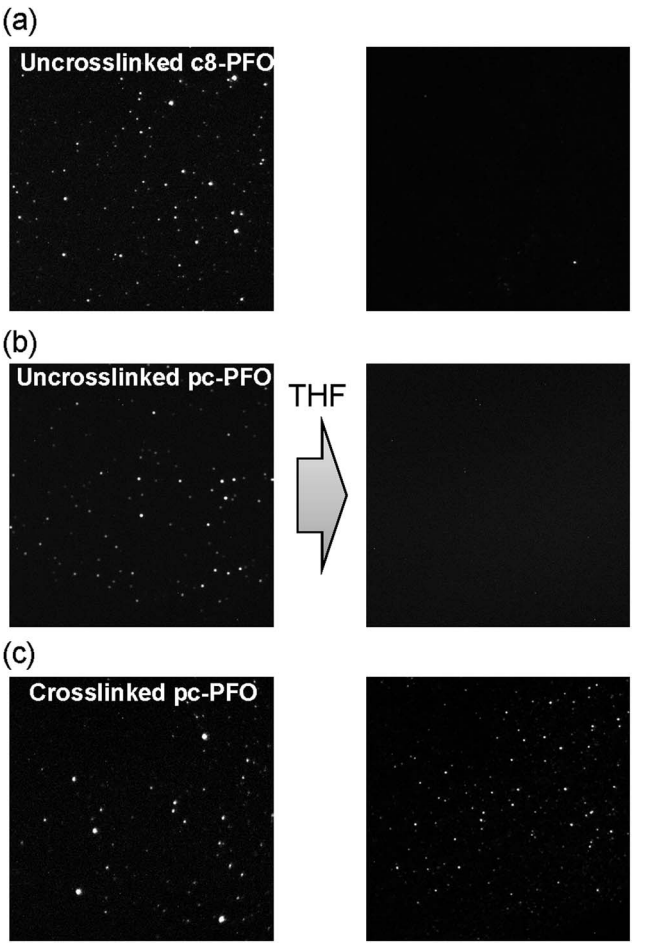

Fig. 5 Fluorescence images of (a) uncrosslinked c8-PFO, (b) uncrosslinked pc-PFO Pdots, and (c) 30 min photocrosslinked pc-PFO Pdots before (left) and after (right) the immersion in THF.

was functionalized with a positive coating using (3-aminopropyl)trimethoxysilane (APTMS). The electrostatic attraction between APTMS and Pdots could stabilize Pdots and attach them firmly onto the glass substrate. After acquiring single-particle images, the Pdot-coated glass substrates were immersed in THF for 30 min at 50 °C to dissolve and wash off non-crosslinked Pdots, after which the Pdot-coated glass substrates were dried for single-particle imaging again.

As shown in Fig. 5, pc-PFO Pdots were attached well on the glass substrate both before (Fig. 5b left) and after (Fig. 5c left) photocrosslinking. We could observe resolved bright single Pdots on the glass substrate under excitation of 405 nm laser light. After immersion in THF solvent, the uncrosslinked pc-PFO Pdots were thoroughly dissolved and thus washed off from the glass substrate, and no bright fluorescent spots could be observed in the single-particle image (Fig. 5b right). Similar phenomena were also observed in c8-PFO Pdots (Fig. 5a left and right), due to good solubility of the uncrosslinked c8-PFO and uncrosslinked pc-PFO Pdots in organic solvents. However, the crosslinked pc-PFO Pdots became quite insoluble in THF even after heating at higher temperature to try to dissolve these crosslinked Pdots. Thus we could observe many bright fluorescent spots left on the glass substrate that corresponded to individual Pdots, as shown in Fig. 5c (right image). This result indicates that crosslinking occurred in the polymer matrix of pc-PFO Pdots after light irradiation, and thus an insoluble 3D intermolecular polymer network formed in pc-PFO Pdots.

Encapsulation of small molecule dye NIR775

Small molecule dye NIR775 was doped in pc-PFO and c8-PFO Pdots, and tested for the potential for the doped dyes to leak out from the Pdots. To examine this leakage, we monitored the normalized NIR fluorescence of 10% NIR775-doped PFO Pdots in aqueous solutions. NIR775 dye was doped in pc-PFO Pdots and c8-PFO, and then doped pc-PFO Pdots were photocrosslinked to test the encapsulating ability of small-molecule dyes. Fig. 6 shows the potential leakage of NIR775 dye from PFO Pdots. By adding 10 vol% THF in Pdot aqueous solution, no significant dye leakage was observed in all Pdot samples (Fig. 6a–c). However, when the THF amount was increased to 200 vol%, NIR775 dye leaked almost completely from uncrosslinked c8-PFO and uncrosslinked pc-PFO Pdots, but NIR775 dye remained in crosslinked pc-PFO Pdots (Fig. 6c and d). We also attempted to use DMSO, which is more biological relevant than THF, but neither untreated nor treated PFO Pdots could dissolve in DMSO.

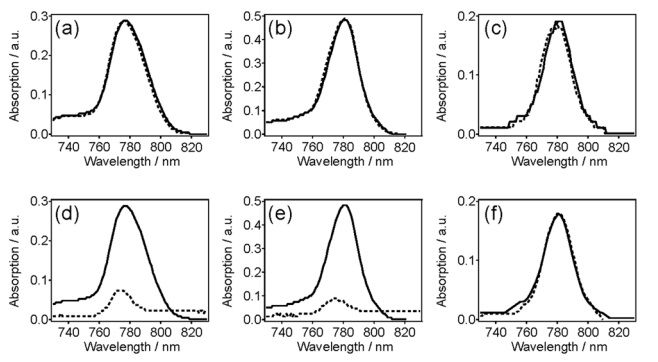

Fig. 6 Leakage studies of NIR775 dye doped in (a and d) uncrosslinked c8-PFO, (b and e) uncrosslinked pc-PFO, and (c and f) crosslinked pc-PFO Pdots. The leakage of 10% NIR dye-doped Pdots was tested by adding (a–c) 10 vol% and (d–f) 200 vol% THF.

These results agree well with the DLS measurements of particle sizes after THF treatments. Adding 10 vol% of THF did not swell significantly the PFO Pdot nanostructure, and they maintained their *ca.* 20 nm particle sizes, and thus NIR775 dye could still remain in all PFO Pdots. However, after adding 200 vol% of THF, NIR775 dye leaked from the solvent swelled uncrosslinked c8-PFO and uncrosslinked pc-PFO Pdots. In contrast, NIR775 dye remained in the crosslinked pc-PFO Pdots as their particle sizes also remained constant after THF treatment as reported by DLS. These results indicate photocrosslinked pc-PFO Pdots were able to maintain their structure and did not get swelled by THF because of the crosslinking of the polymer network in the Pdots. The crosslinked polymer network also prevented the leakage of the encapsulated small molecule dye.

We note photobleaching of NIR775 dyes occurred (~40% decrease based on UV-vis spectra) during UV irradiation and photocrosslinking. However, the purpose of this study was to determine the ability of the crosslinked Pdots to retain small molecules and provide stable encapsulation without leakage, and for this, NIR775 served as a convenient model as leakage was easily monitored *via* fluorescence. The ability of photocrosslinked Pdots to retain small molecules may be particularly applicable to non-fluorescent molecules, as Pdots are also being explored for drug delivery applications because their hydrophobic interior is well suited for hosting many drugs that are hydrophobic. For these applications, photobleaching would not be a concern. Finally, even for fluorescent molecules, such as NIR775, a decrease in 40% of the signal may still result in a bright probe as we have shown Pdots can be up to 30× brighter than Qdots.[3]

Flow cytometry

To validate whether Pdots can be used as fluorescent probes for cellular labeling, we performed bioconjugation of streptavidin to the uncrosslinked and crosslinked pc-PFO Pdots, and demonstrated specific cell surface labeling using the Pdot-bioconjugates (details in Experimental section). The streptavidin conjugated Pdots were labeled to the cell surface through biotinylated primary anti-EpCAM antibody. The pc-PFO Pdots were photocrosslinked before bioconjugation and labeling of the MCF-7 cells. MCF-7 cells were then incubated in a blocking buffer with each type of pc-PFO Pdots of the same diameter (18 nm) at the same concentration (25 nM) for 30 min. The cells were then washed twice before the flow experiments. Fig. 7 shows the flow cytometry results of the cells incubated with uncrosslinked pc-PFO Pdots (black and grey) and after photocrosslinking for 30 min (blue and light blue) and 60 min (red and orange), respectively. As shown by the flow cytometry

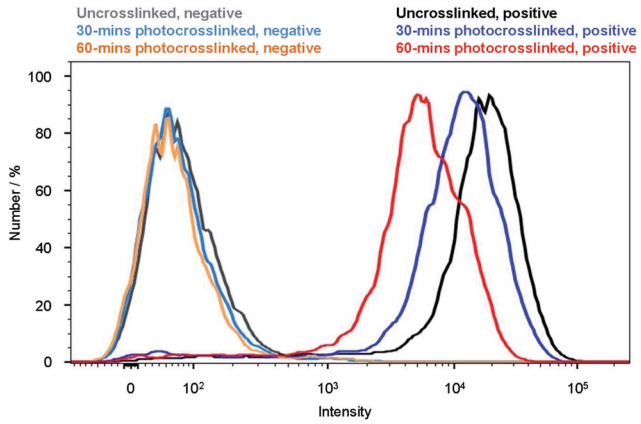

Fig. 7 Flow cytometry measurements of the intensity distributions of MCF-7 breast cancer cells labeled *via* nonspecific binding (negative control performed in the absence of biotinylated primary antibodies; solid lines on the left) and positive specific targeting (solid lines on the right) of pc-PFO Pdots for uncrosslinked (black for positive and grey for negative), 30 min photocrosslinked (blue for positive and light blue for negative) and 60 min photocrosslinked (red for positive and orange for negative) Pdots.

results, the fluorescence intensity of MCF-7 cells incubated with pc-PFO Pdots after photocrosslinking for 30 min decreased slightly but still maintained an excellent specific cell labeling ability. However, MCF-7 cells incubated with pc-PFO Pdots after photocrosslinking for too long (60 min) showed a rapid decrease in cell fluorescence intensity due to the photobleaching of Pdots and the decrease in quantum yield caused by light irradiation. Flow cytometry of c8-PFO Pdots incubated with MCF-7 cells were also performed, and c8-PFO Pdots showed a similar trend in cell-labeling-brightness decrease with increasing irradiation time (Fig. S4†). pc-PFO Pdots showed comparable specific cellular targeting capability as c8-PFO Pdots, while crosslinked pc-PFO Pdots formed by 30 min light irradiation also exhibited excellent specific cellular targeting capability.

Conclusions

This paper describes a synthetic approach for photocrosslinkable semiconducting polymer dots, and demonstrates their superior ability to crosslink and form 3-D intermolecular polymer networks. This strategy offers some important advantages: (1) photocrosslinking provides a remote method for controlling Pdot properties; (2) crosslinked Pdots showed enhanced colloidal stability, as well as enhanced physical and chemical stability; (3) crosslinked Pdots can be utilized as efficient small-molecule capsules for creating functional materials; (4) crosslinked Pdots can act as a promising cell labeling fluorophore for biological applications. This study demonstrates photocrosslinking can enhance Pdot stability against dissociation, although it does not address the colloidal stability against aggregation. For this latter point, the surface of Pdots plays a more important role as discussed in our previous reports.[5,28] Considering optical stimulus can work remotely and non-invasively, this study should stimulate additional work in this area for further development of stimuli-responsive ultrabright and versatile Pdot probes.

Author contributions

D.T.C. initiated the project; Y.Z. and D.T.C designed the experiments; Y.Z. synthesized the polymers, performed the experiments and wrote the paper; F.Y. helped the overall characterization of Pdots, flow measurement and fluorescence microscope experiments and modified the manuscript. W.S. conducted TEM and helped fluorescence microscope experiments; J.Y., I.W., Y.Z., and Y.R. helped to interpret the results and carried out characterization of the polymers. The manuscript was written through contributions of all authors. All authors have given approval to the final version of the manuscript.

Acknowledgements

D.T.C gratefully acknowledges support of this work by the National Institutes of Health (R21CA186798 and R01NS052637).

Notes and references

1 C. Wu, B. Bull, C. Szymanski, K. Christensen and J. McNeill, *ACS Nano*, 2008, **2**, 2415–2423.
2 C. Wu, Y. Jin, T. Schneider, D. R. Burnham, P. B. Smith and D. T. Chiu, *Angew. Chem., Int. Ed.*, 2010, **49**, 9436–9440.
3 C. Wu, T. Schneider, M. Zeigler, J. Yu, P. G. Schiro, D. R. Burnham, J. McNeill and D. T. Chiu, *J. Am. Chem. Soc.*, 2010, **132**, 15410–15417.
4 K. Pu, A. J. Shuhendler, J. V. Jokerst, J. Mei, S. S. Gambhir, Z. Bao and J. Rao, *Nat. Nanotechnol.*, 2014, **9**, 233–239.
5 C. Wu and D. T. Chiu, *Angew. Chem., Int. Ed.*, 2013, **52**, 3086–3109.
6 A. Kaeser and A. P. H. J. Schenning, *Adv. Mater.*, 2010, **22**, 2985–2997.
7 E. S. Childress, C. A. Roberts, D. Y. Sherwood, C. L. M. LeGuyader and E. J. Harbron, *Anal. Chem.*, 2012, **84**, 1235–1239.
8 Y.-J. Ko, E. Mendez and J. H. Moon, *Macromolecules*, 2011, **44**, 5527–5530.
9 J. Pecher and S. Mecking, *Chem. Rev.*, 2010, **110**, 6260–6279.
10 K. Petkau, A. Kaeser, I. Fischer, L. Brunsveld and A. P. H. J. Schenning, *J. Am. Chem. Soc.*, 2011, **133**, 17063–17071.
11 F. Schuetze, B. Stempfle, C. Juengst, D. Woell, A. Zumbusch and S. Mecking, *Chem. Commun.*, 2012, **48**, 2104–2106.
12 C. Wu, S. J. Hansen, Q. Hou, J. Yu, M. Zeigler, Y. Jin, D. R. Burnham, J. D. McNeill, J. M. Olson and D. T. Chiu, *Angew. Chem., Int. Ed.*, 2011, **50**, 3430–3434.
13 K.-Y. Pu, K. Li and B. Liu, *Chem. Mater.*, 2010, **22**, 6736–6741.
14 F. Ye, C. Wu, Y. Jin, M. Wang, Y.-H. Chan, J. Yu, W. Sun, S. Hayden and D. T. Chiu, *Chem. Commun.*, 2012, **48**, 1778–1780.

15 E. Ahmed, S. W. Morton, P. T. Hammond and T. M. Swager, *Adv. Mater.*, 2013, **25**, 4504–4510.
16 K. Pu and B. Liu, *Adv. Funct. Mater.*, 2011, **21**, 3408–3423.
17 K. Pu, A. J. Shuhendler and J. Rao, *Angew. Chem., Int. Ed.*, 2013, **52**, 10325–10329.
18 A. J. Shuhendler, K. Pu, L. Cui, J. P. Uetrecht and J. Rao, *Nat. Biotechnol.*, 2014, **32**, 373–380.
19 J. Yu, C. Wu, X. Zhang, F. Ye, M. E. Gallina, Y. Rong, I. C. Wu, W. Sun, Y.-H. Chan and D. T. Chiu, *Adv. Mater.*, 2012, **24**, 3498–3504.
20 Y. Rong, C. Wu, J. Yu, X. Zhang, F. Ye, M. Zeigler, M. E. Gallina, I. C. Wu, Y. Zhang, Y.-H. Chan, W. Sun, K. Uvdal and D. T. Chiu, *ACS Nano*, 2013, **7**, 376–384.
21 Y.-H. Chan, C. Wu, F. Ye, Y. Jin, P. B. Smith and D. T. Chiu, *Anal. Chem.*, 2011, **83**, 1448–1455.
22 F. Ye, C. Wu, Y. Jin, Y.-H. Chan, X. Zhang and D. T. Chiu, *J. Am. Chem. Soc.*, 2011, **133**, 8146–8149.
23 Y.-H. Chan, Y. Jin, C. Wu and D. T. Chiu, *Chem. Commun.*, 2011, **47**, 2820–2822.
24 Y.-H. Chan, M. E. Gallina, X. Zhang, I. C. Wu, Y. Jin, W. Sun and D. T. Chiu, *Anal. Chem.*, 2012, **84**, 9431–9438.
25 E. Hittinger, A. Kokil and C. Weder, *Angew. Chem., Int. Ed.*, 2004, **43**, 1808–1811.
26 L. Zhou, J. Geng, G. Wang, J. Liu and B. Liu, *ACS Macro Lett.*, 2012, **1**, 927–932.
27 C. Wu and J. McNeill, *Langmuir*, 2008, **24**, 5855–5861.
28 Y. Jin, F. Ye, C. Wu, Y.-H. Chan and D. T. Chiu, *Chem. Commun.*, 2012, **48**, 3161–3163.